Int. J. Nanosci. Nanotechnol., Vol. 15, No. 4, Dec. 2019, pp. 265-275

Short Communication

Modeling of Nanofiltration for Concentrated Electrolyte Solutions using Linearized Transport Pore Model

Morteza Sepehrinia and Mohammad Mahdi Zerafat*

Department of Nanochemical Engineering, Faculty of Advanced Technologies, Shiraz University, P.O.Box 7194684560, Shiraz, Iran.

(*) Corresponding author: mmzerafat@shirazu.ac.ir
(Received: 19 November 2018 and Accepted: 26 December 2018)

Abstract

In this study, linearized transport pore model (LTPM) is applied for modeling nanofiltration (NF) membrane separation process. This modeling approach is based on the modified extended Nernst-Planck equation enhanced by Debye-Huckel theory to take into account the variations of activity coefficient especially at high salt concentrations. Rejection of single-salt (NaCl) electrolyte is investigated to take into account the effect of feed concentration, membrane charge density and pore size on rejection. The results show that the reduction of feed concentration and membrane pore size lead to increase the rejection of electrolyte in NF separation process. Furthermore, increasing the membrane charge density causes the rejection of co-ions to be increased leading to an enhanced total rejection. LTPM is compared to unmodified linearized model which approves the higher precision of the modified model especially at higher concentrations.

Keywords: *LTPM, Modified extended Nernst-Planck equation, Debye-Huckel.*

1. INRODUCTION

Nanofiltration is utilized in various industrial and environmental applications due to lower energy consumption and higher flux compared with reverse osmosis [1]. Modeling of NF separation for prediction of membrane performance and also a proper understanding of background mechanisms involved have been considered extensively in recent decades. Several fabrication techniques containing experimental data on the subject have been published during last decades [2, 3]. Also, during the last decade, modeling approaches have been redirected from black box empirical models based on irreversible thermodynamics to models based on enhanced Nernst planck (ENP). ENP_based models supply information on membrane properties and flow characteristics, incorporating the physical reality of the membrane in order to match measurable quantities like flux and rejection with adjustable membrane parameters such as membrane pore size, pore size distribution, membrane charge, thickness and etc. The most serious limitation in NF modeling is the requirement for the determination of model parameters like membrane charge and pore size which are not measurable easily in dimensions substantially close to atomic scales. Nanoscale phenomena involved in NF separation mechanisms for charged moieties are very complex. As a result, development of more accurate physical models (like molecular dynamic simulation) is also considered due to the absence of precise information on the physical structure and electrical properties of real NF membranes [4]. So,

development of NF modeling entails improvement of measurement methods for characterization of NF membranes and process flows so that a proper investigation according to model parameters becomes possible.

Table 1. *Advantages and disadvantages of each modeling approach.*

Model	Advantages	Disadvantages
SC [1]	Radial mass transport is considered	Complexity of equations
TMS [1]	Simplicity compared with SC	Radial mass transport is ignored
DSPM [5-10]	Porous membranes, considering steric effects	Ignoring donnan and dielectric effects
DSPM-DE [11-15]	Including donnan & dielectric effects	Complexity and time consuming procedure for solving equations
LTM [16, 17]	Reduction of the system of equations from differential equations to a system of algebraic equations and thus ease of solution.	Ignoring the effect of activity coefficient in ENP
MENP [18,19]	Considering all effective parameters in the model	Higher complexity of the system of equations
HM [20]	Higher prediction capability compared with SC & TMS	Limited to homogeneous non-porous membranes

Various continuum modeling approaches are implemented for the modeling of NF each with variable degrees of accuracy including ENP_based models like DSPM [5-10], DSPM-DE [11-15], LTM [16, 17] and MENP [18,19], and also SC [1], TMS [1], HM [20], SEDE [21-23], SEDE-VCh [24] and PPTM [25-28]. A list of advantages and disadvantages of each modeling approach is summarized in Table 1.

In this study, linearized transport pore model (LTPM) is applied for modeling NF separation process for a single-salt NaCl electrolyte. This modeling approach is based on the modified extended Nernst-Planck equation enhanced by Debye-Huckel theory to take into account the variations of activity coefficient at high salt concentrations, the details of which can be found in our previous study [18, 19]. The difference between the approach in this study and our previous model is based in the application of linearization which reduces the calculation load of equations. This gives the model the potential for industrial calculations with a still acceptable precision. Rejection of single-salt (NaCl) electrolyte is investigated to take into account the effect of feed concentration, membrane charge density and pore size on flux and rejection. Based on the results, modified LTPM shows a good alternative for NF modeling within low to moderate feed concentration ranges.

2. LINEARIZED TRANSPORT PORE MODEL (LTPM)

The extended Nernst-Planck (ENP) which is the governing equation for steady-state flux (Ji) of charged species through membrane pores takes into account the contributions of diffusion, convection and electrical migration in the total ionic flux as follows:

$$J_i = K_{i,c} c_i J_v - D_{i,p}\left[\begin{array}{l}\mathrm{grad}\left(c_i\right)+\frac{z_i c_i F}{RT}\mathrm{grad}\left(\psi\right)+\\ c_i\,\mathrm{grad}\left(\ln\gamma_i\right)+\frac{c_i v_i}{RT}\mathrm{grad}\left(P\right)\end{array}\right] \qquad (1)$$

Where, Di,p is the ionic hindered diffusivity inside the pores and Ki,c the convective hindrance factor. Pressure differential is generally ignored in previous modeling studies. The influence of activity coefficient gradient is also ignored except for MENP model based on the assumption of dilute feed which is certainly deviated in stronger electrolyte solutions. For a single salt like NaCl, the gradient of electrical potential can be re-written as follows:

$$\frac{d\psi}{dx}=\frac{\frac{z_1V}{D_{1,p}}(K_{1,c}-C_{1,p})+\frac{z_2V}{D_{2,p}}(K_{2,c}-C_{2,p})}{\frac{F}{RT}(z_1^2c_1+z_2^2c_2)} \qquad (2)$$

Eq. 2 is linearized so that it gives:

$$\left(\frac{K_{1,c}V}{D_{1,p}}+\frac{K_{2,c}V}{D_{2,p}}\right)c_{1,av}^2+\left[\left(\frac{K_{1,c}V}{D_{1,p}}+\frac{K_{2,c}V}{D_{2,p}}\right)X_d-\left(\frac{V}{D_{1,p}}+\frac{V}{D_{2,p}}\right)C_p\right]c_{1,av} \qquad (3)$$

$$\frac{\Delta c_1}{\Delta x}=\frac{-\frac{V}{D_{1,p}}X_dC_p}{2c_{1,av}+X_d}$$

This can be simplified by description of the non-dimensional peclet number as follows:

$$Pe_i=\frac{K_{i,c}V\Delta x}{D_{i,p}}=\frac{K_{i,c}\Delta x}{D_{i,p}}\left(\frac{r_p^2\Delta P_e}{8\eta\Delta x}\right)=\frac{K_{i,c}r_p^2\Delta P_e}{8D_{i,p}\eta} \qquad (4)$$

Rewriting Eq. 3 for Cp results in the following relation:

$$C_p=\frac{(Pe_1+Pe_2)c_{1,av}^2+(Pe_1+Pe_2)X_dc_{1,av}-(2c_{1,av}+X_d)\Delta c_1}{\left(\frac{Pe_1}{K_{1,c}}+\frac{Pe_2}{K_{2,c}}\right)c_{1,av}+\frac{Pe_1}{K_{1,c}}X_d} \qquad (5)$$

Partition coefficients are needed to calculate $c_{1,av}$ to relate the inter-pore and intera-pore concentrations:

$$\frac{c_i(0^+)}{c_i(0^-)}=\varphi_i\frac{\gamma_i(0^-)}{\gamma_i(0^+)}\exp\left(\frac{-\Delta W_i}{k_BT}\right)\exp\left(-\frac{z_iF}{RT}\Delta\psi_D\right) \qquad (6)$$

The results will be:

$$c_1(0)=\frac{-X_d+\sqrt{X_d^2+4\Phi_1'\Phi_2'C_w^2}}{2} \qquad (7)$$

$$c_1(\Delta x)=\frac{-X_d+\sqrt{X_d^2+4\Phi_1'\Phi_2'C_p^2}}{2} \qquad (8)$$

$$c_{1,av}=\frac{c_1(\Delta x)+c_1(0)}{2} \qquad (9)$$

$$\Delta c_1=c_1(\Delta x)-c_1(0) \qquad (10)$$

Linearization results in the reduction of the total system to three independent equations with $c_1(0)$, $c_1(\Delta x)$ and C_p as the unknown variables. The following algorithm can be used for solving the system of equations:

(1) $c_1(0)$ is calculated using Eq. 7 by at a fixed feed concentration (C_w).

(2) C_p is guessed and $c_1(\Delta x)$ is calculated using Eq. 8.

(3) $c_{1,av}$ and Δc_1 are calculated using Eq. 9 and the guessed value is compared to Eq. 10.

(4) Iteration is performed in the $0 \le C_p \le C_w$ range until convergence is prevailed.

(5) Rejection is calculated using $R = 1 - C_p / C_w$.

MENP modeling approach was proposed by Zerafat et al. for the transport of high ionic strength NaCl electrolyte based on modified Nernst-Planck equation. Based on the results, the effect of ionic strength on gradient of activity coefficient cannot be ignored at high ionic strength values [18, 19]. In this study, LTPM and MENP modeling approaches are combined for modeling NF separation to take into account the effect of high ionic strength on rejection by reducing the complexity of the equations at the same time.

3. LTPM-MENP MODELING

3.1 Rejection of Single Salt Solutions

Ignoring the effect of activity coefficient in the NF of concentrated electrolyte solutions is not a proper assumption which results in the reduction of precision in the predicted rejection values especially at high feed concentrations. Activity coefficient of an ion is a simple or

complicated function of ionic strength in the electrolyte solution [1]. Some prevalent equations relating activity coefficient to ionic strength are summarized in Table 2. Also, Fig. 1 shows the variations of these equations with concentration which exhibits a significant controversy especially at higher ionic strength values.

***Table 2**. Activity Coefficient correlations as a function of Ionic Strength.*

Model	Formulation	Coefficients	Features
Debye-Huckel	$\ln(\gamma_i) = -Az_i^2\sqrt{I}$	$A(T) = \frac{\sqrt{2}F^2 e_0}{8T(\varepsilon RT)^{3/2}}$	Ions are assumed as point charges occupying no volume
Extended Debye-Huckel	$\ln(\gamma_i) = \frac{-Az_i^2\sqrt{I}}{1+(Br_i\sqrt{I})}$	$A = F\sqrt{\frac{2}{\varepsilon_0\varepsilon_r RT}}$ $B = \frac{e^2 F}{4\sqrt{2}\ln 10(\varepsilon_0\varepsilon_r RT)^{3/2}}$	The volume occupied by ions is taken into account
Davies Eq.	$\ln(\gamma_i) = -Az_i^2\left(\frac{\sqrt{I}}{1+\sqrt{I}} - 0.3I\right)$	$A(T) = \frac{e_0^3 N_A^{1/2}}{\ln 10 \times 4\pi\sqrt{2} \times (\varepsilon^3 k_B^3 T^3)^{1/2}}$	Semi-Concentrated Multi-Component Ionic Solutions (Semi-empirical)

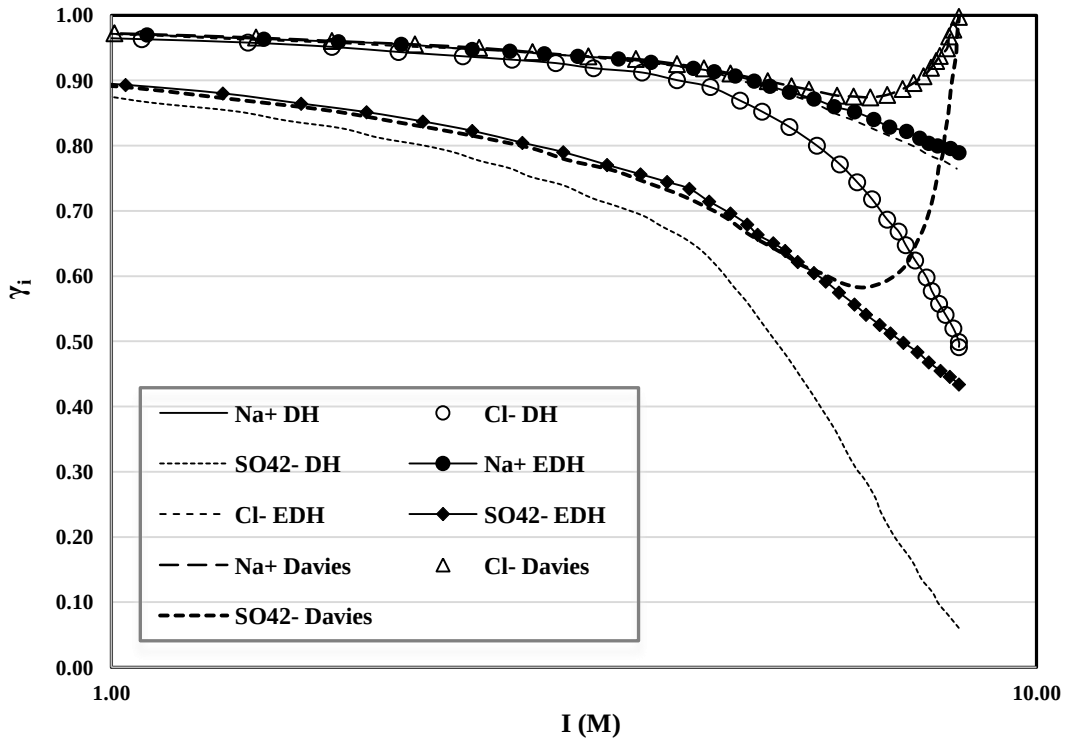

***Figure 1.** Variations of activity coefficient with concentration based on Debye-Huckel, Extended Debye-Huckel and Davies Equations.*

Eq. 2 turns into the following equation by taking into account the variations of activity coefficient:

$$\frac{d\psi}{dx} = \frac{\alpha(I)\left[\frac{V}{D_{1,p}}\left[K_{1,c}c_1 - C_{1,p}\right]\right] + \beta(I)\left[\frac{V}{D_{2,p}}\left[K_{2,c}c_2 - C_{2,p}\right]\right]}{\gamma(I)\frac{F}{RT}} \qquad (11)$$

Where,

$$\alpha(I) = 4\sqrt{I}z_1 - Az_1z_2^4c_2 + Az_1^2z_2^3c_2$$
$$\beta(I) = 4\sqrt{I}z_2 - Az_2z_1^4c_1 + Az_2^2z_1^3c_1$$
$$\gamma(I) = 4\sqrt{I}(z_1^2c_1 + z_2^2c_2) - Az_1^2z_2^2c_1c_2(z_1^2 + z_2^2) + 2Az_1^3z_2^3c_1c_2 \quad (12)$$

For NaCl and Na_2SO_4, these will be:

$$\alpha(I) = 4\sqrt{I} - 2Ac_2$$
$$\beta(I) = -4\sqrt{I} + 2Ac_1 \quad \text{NaCl} \quad (13)$$
$$\gamma(I) = 4\sqrt{I}(c_1 + c_2) - 4Ac_1c_2$$

$$\alpha(I) = 4\sqrt{I} - 24Ac_2$$
$$\beta(I) = -8\sqrt{I} + 6Ac_1 \quad \text{Na}_2\text{SO}_4 \quad (14)$$
$$\gamma(I) = 4\sqrt{I}(c_1 + 4c_2) - 36Ac_1c_2$$

Equilibrium dissociation by taking into account the variation of activity coefficient will be:

$$\frac{c_i}{C_i} = \varphi_i \frac{\Gamma_i}{\gamma_i} \exp\left(\frac{-\Delta W_i}{k_B T}\right) \exp\left(-\frac{z_i F}{RT}\Delta\Psi_D\right) \quad (15)$$

By defining:

$$\varphi_i' = \varphi_i \exp\left(\frac{-\Delta W_i}{k_B T}\right) \quad (16)$$

$$\Delta\Psi_D = -\frac{RT}{z_i F}\ln\left(\frac{c_i\gamma_i}{C_i\Gamma_i\varphi_i'}\right) \quad (17)$$

Based on Debye-Huckel theory, the activity of each ion in the solution is given by:

$$\gamma_i = \exp -Az_i^2\left(0.5\sum_i z_i^2 c_i\right)^{0.5} \quad (18)$$

For a single salt electrolyte, the interpore and inrapore activity coefficients are:

$$\Gamma_i = \exp\left(-Az_i^2\sqrt{0.5(z_1^2C_1 + z_2^2C_2)}\right) \quad \text{(intra-pore)} \quad (19)$$

$$\gamma_i = \exp\left(-Az_i^2\sqrt{0.5(z_1^2c_1 + z_2^2c_2)}\right) \quad \text{(inter-pore)} \quad (20)$$

So, inter-pore and intra-pore Donnan potential values are:

$$\Delta\Psi_{1,D}(0) = \Delta\Psi_{2,D}(0) \quad \therefore$$
$$\frac{1}{z_1}\ln\left(\frac{c_1(0)\gamma_1(0)}{C_{1,w}\Gamma_1\varphi_1'}\right) = \frac{1}{z_2}\ln\left(\frac{c_2(0)\gamma_2(0)}{C_{2,w}\Gamma_2\varphi_2'}\right) \quad (21)$$

For the special case of 1:1 electrolytes:

$$c_2(0) = c_1(0) + X_d$$
$$\gamma_1(0) = \exp -A\sqrt{c_1(0) + 0.5X_d} = \gamma_2(0) \quad (22)$$
$$\Gamma_1 = \exp -A\sqrt{C_w} = \Gamma_2$$

Which results in:

$$\left[c_1^2(0) + c_1(0)X_d\right]\exp\left(-2A\sqrt{c_1(0) + 0.5X_d}\right) - C_w^2\varphi_1'\varphi_2'\exp\left(-2A\sqrt{C_w}\right) = 0 \quad (23)$$

This equation is solved based on Newton-Raphson procedure to obtain $c_1(0)$.

3.2 Simulated Annealing

Simulated annealing algorithm is a powerful stochastic search method which is used to find a proper solution not necessarily optimized for combinatorial problems [29]. In combinatorial problems, a combination of some parameters and their permutation is proposed [30].

The idea behind simulated annealing is based on the annealing process. In the annealing process an alloy like steel is heated up to a certain temperature and after a certain period is cooled to the ambient temperature. The microstructure of annealed components are at equilibrium and pseudo-equilibrium state due to sufficient time for cooling and possess the minimum energy level. The energy distribution of the components at each temperature follows Maxwell-Boltzmann probability function:

$$P(E) \sim \exp\left(\frac{-E}{k_B T}\right) \quad (24)$$

In this technique, a high initial temperature is presumed for the system and then reducing this temperature to a lower value which is often the ambient temperature, through stochastic search in the neighborhood and utilizing Maxwell-

Boltzmann probability distribution function the optimal value is determined in the acceptable range of parameters [31]. The effective parameters in simulated annealing are**:**

1. **Starting point:** An acceptable answer that is generated randomly and affects the convergence rate of the algorithm.
2. **Initial temperature**: This should be chosen so that the Maxwell-Boltzmann probability distribution function for initial random inputs produce a value close to unity.
3. **Temperature reduction rate**: Normally, 0.85-0.95 is desirable. The large values of this parameter prolong the runtime and extend the search space, while very small amounts of cooling may cause early algorithmic convergence.
4. **The number of repetitions in the inner loop**: Low values lead to convergence to local optima and increase the rate of convergence. Therefore, the value of this parameter must be large enough to produce a large number of solutions to create a thermal equilibrium at any temperature.

The value of these parameters depend on the dimensions of the problem and with several times the test run of the algorithm is determined for different values [32].

4. RESULTS AND DISCUSSION

The combination of transport and partitioning equations (Eqs.1-10), are solved using simulated annealing technique. The governing equations for NF membrane separation are solved using LTPM and the results are compared with the results from MENP. Numerical integration of ENP is performed using 4^{th} order Runge-Kutta method with h = 0.01 as the step size.

4.1 Rejection of Single Salt Electrolytes

The results for the rejection of single salt (NaCl) electrolytes are given and compared in Tables 3-5 which are solved based on LTPM and MENP, respectively. For single electrolytes of a 1:1 salt (NaCl), it should be mentioned that the rejection of both ions will be the same. So, for every solution calculation of the rejection value of one ion is sufficient. The effects of various parameters such as feed concentration, membrane charge and pore size are also investigated on ionic rejection. Based on Tables 3-5, LTPM has always a higher prediction for rejection compared with MENP with different error percent in the 1.5-18.9 % range. Also, Fig. 2 shows the variations of rejection at various transmembrane pressures and feed concentrations. It is obvious that after a certain feed concentration (0.1 M) transmembrane pressure enhancement cannot increase the rejection significantly.

Table 3. *Comparison of rejection values for NaCl solution by MENP and LTPM models (X_d = - 0.001 M, ΔP_e = 5 bar).*

C_w (M)	r_p (nm)	MENP	LTPM	Error %
		Rejection %		
0.001	0.5	0.8840	0.9232	4
0.001	1	0.2650	0.2974	10.9
0.001	2	0.1623	0.1748	7.1
0.01	0.5	0.4161	0.5136	18.9
0.01	1	0.1342	0.1463	8.3
0.01	2	0.1124	0.12	6.3
0.1	0.5	0.3646	0.4167	12.5
0.1	1	0.1403	0.1528	8.2
0.1	2	0.1171	0.1248	6.2
١	0.5	0.3758	0.4302	12.6
1	1	0.1412	0.1539	8.2
1	2	0.1176	0.1254	6.2

Table 4. *Comparison of rejection values for NaCl solution by MENP and LTPM models (X_d = - 0.001 M, ΔP_e = 15 bar).*

C_w (M)	r_p (nm)	MENP	LTPM	Error %
		Rejection %		
0.001	0.5	0.9577	0.9722	1.5
0.001	1	0.5332	0.5775	7.6
0.001	2	0.3283	0.3609	9
0.01	0.5	0.7003	0.7787	10
0.01	1	0.2997	0.3220	6.9
0.01	2	0.2331	0.2510	7.1
0.1	0.5	0.6210	0.6724	7.6

0.1	1	0.3109	0.3335	6.7
0.1	2	0.2416	0.26	7
١	0.5	0.6340	0.6849	7.4
1	1	0.3127	0.3355	6.8
1	2	0.2427	0.2612	7

Table 5. *Comparison of rejection values for NaCl solution by MENP and LTPM models (X_d = - 0.001 M, ΔP_e = 25 bar).*

C_w (M)	r_p (nm)	MENP	LTPM	Error %
		Rejection %		
0.001	0.5	0.9726	0.9821	0.9
0.001	1	0.2650	0.2974	12.2
0.001	2	0.1623	0.1748	8.9
0.01	0.5	0.7965	0.8536	6.7
0.01	1	0.1342	0.1463	4.4
0.01	2	0.1124	0.12	4
0.1	0.5	0.7234	0.7673	5.7
0.1	1	0.1403	0.1528	4.7
0.1	2	0.1171	0.1248	5
١	0.5	0.7349	0.777	5.4
1	1	0.1412	0.1539	4.6
1	2	0.1176	0.1254	4.3

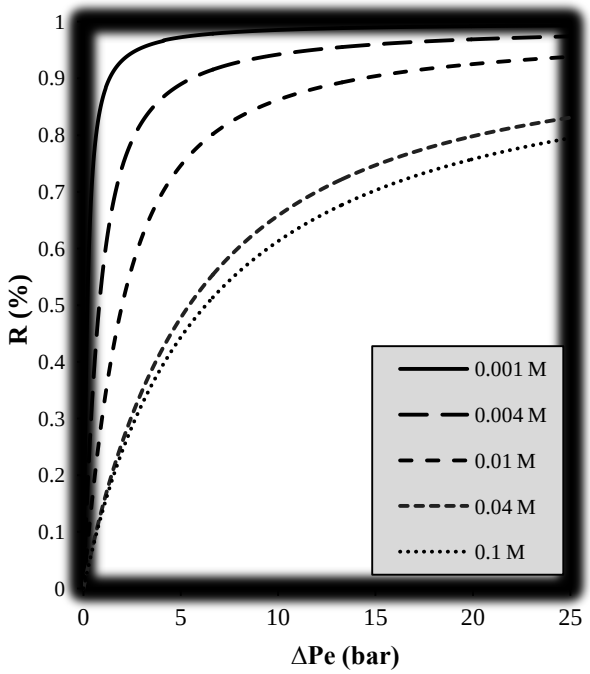

Figure 2. *Variations of Rejection for NaCl solution as a function of pressure differential for various feed concentrations using 3-parameter LTPM (r_p = 0.45 nm).*

4.2 Effect of Feed Concentration

Fig. 3 shows the rejection values for a single salt solution of NaCl for various feed concentrations using LTPM approach. Based on the results, rejection is reduced rapidly with concentration and maintains a constant value at ~ 0.01 M.

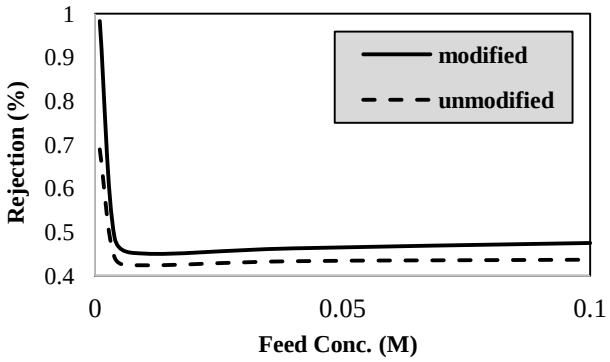

Figure 3. *Effect of feed concentration of the rejection of NaCl for LTPM and modified LTPM.*

Based on this figure, the modified model has always a higher prediction of rejection. This can be due to the effect of intermolecular forces which reflect themselves in the activity coefficient and higher interactions with the membrane material resulting in higher rejections at similar feed concentrations.

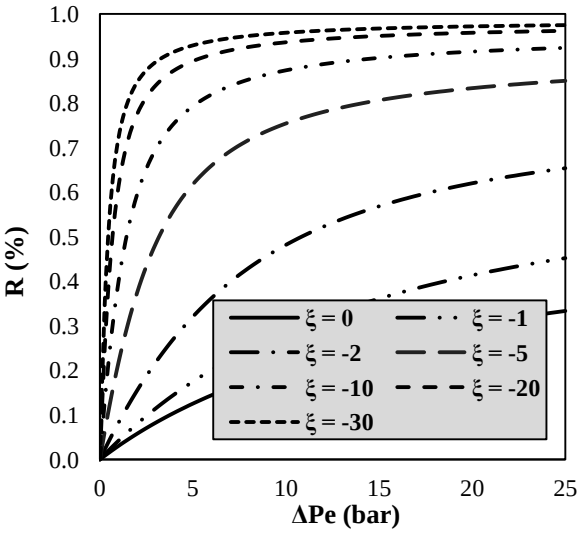

Figure 4. *Variations of NaCl rejection as a function of transmembrane pressure at different membrane charge densities using the 3 parameter LTPM (r_p = 2 nm).*

4.3 Effect of Membrane Charge

Fig. 4 shows the effect of NaCl rejection as a function of transmembrane pressure at various membrane charge values. As it is obvious, the sign and value of membrane charge has a significant effect on rejection

increasing by increasing the membrane charge. It should be noted that charge exclusion is one of the main rejection mechanisms contributing in NF separation. Based on this mechanism, repulsion of ions with same charge as the membrane prevents ions from passing through membrane pores.

4.4 Effect of Pore Size

Fig. 5 presents the variations of rejection as a function of transmembrane pressure at various pore size values. Based on this figure, the smaller the membrane pores the higher the rejection is where at 0.5 nm the rejection is enhanced significantly, which is the initiation of RO behavior. Fig. 6 also shows the variations of rejection as a function of pore size compared for the modified and unmodified versions of LTPM model. The results show that the variation of ionic strength show a more significant impact on rejection at higher pore radii where they approach the same value at small pore radii close to ~ 0.5 nm.
For investigating the precision of linearization, the numerical solution by Runge-Kutta method is compared with the linearized results. For NaCl, the results of concentration profile across the membrane for various pore sizes and membrane charge values are given in Figs. 7 (a)-(d). Based on Figs. 7 (a)-(d), the linear assumption seems to be acceptable at low concentrations. The rejection values for NaCl solution are given in Tables 1 to 3 at 1, 10 and 25 bar. The results show that at low pressures the linearized model has a good accordance with the full model while at higher pressures the error is intensified (especially at low concentrations).

4.5 Effect of Activity Coefficient

Effect of activity coefficient variations on the rejection of single salt solutions is investigated by comparing the results based on ENP and MENP models for NaCl solution.

Based on the results in Tables 6-8, at low pressures (under ~ 10 bar) ignoring activity coefficient doesn't introduce serious faults in the predicted values while at higher pressures (> ~ 10 bar) the effect of activity coefficient variation on rejection cannot be ignored especially at 2 nm pore size which is considered as the nominal upper limit of NF behavior in pressure-driven membrane separation processes.

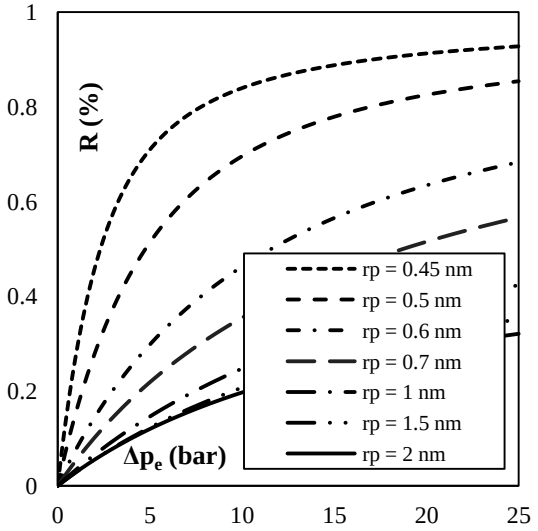

Figure 5. *The variations of rejection for NaCl solution as a function of transmembrane pressure for various pore size values using the 3-parameter LTPM model.*

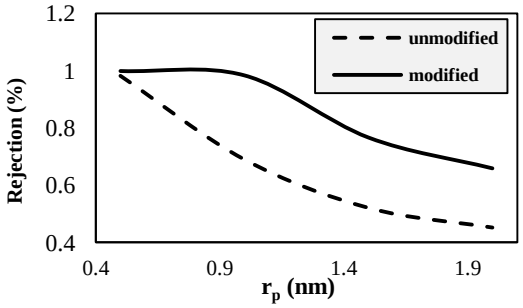

Figure 6. *Variations of rejection as a function of pore size compared for modified and unmodified versions of LTPM model.*

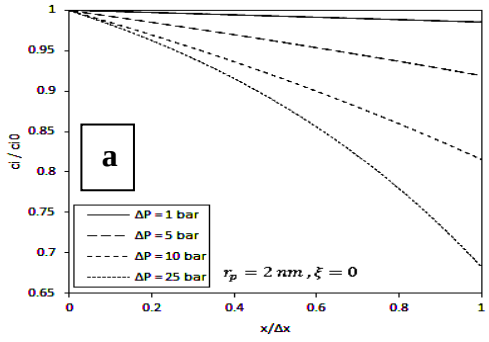

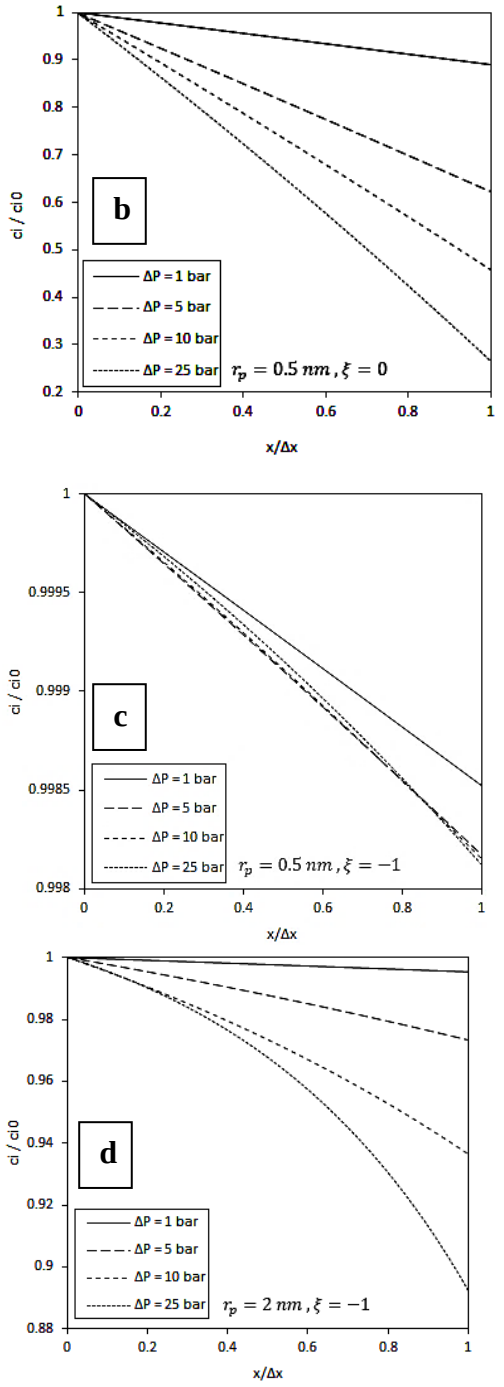

Figure 7*. The profiles of dimensionless concentration of Na^+ using the 3-paramter LTPM model:* ***(a)*** *r_p=2 nm, X_d =0,* ***(b)*** *r_p = 0.5 nm, X_d = -1,* ***(c)*** *r_p = 0.5 nm, X_d=0, and* ***(d)*** *r_p=2 nm, X_d = -1.*

Table 6. *Comparison of rejection values for NaCl solution (X_d = - 0.001 M, ΔP_e = 1 bar).*

C_w (M)	r_p (nm)	MENP	ENP	Error %
		Rejection %		
0.001	0.5	0.9847	0.6670	32.3
0.001	1	0.1617	0.0725	55.2
0.001	2	0.0689	0.0421	38.9
0.01	0.5	0.1513	0.1566	3.4
0.01	1	0.0367	0.0343	6.5
0.01	2	0.0408	0.029	28.9
0.1	0.5	0.1245	0.1275	2.3
0.1	1	0.0405	0.0359	11.3
0.1	2	0.0433	0.0303	30

Table 7. *Comparison of rejection values for NaCl solution (X_d = - 0.001 M, ΔP_e = 10 bar).*

C_w (M)	r_p (nm)	MENP	ENP	Error %
		Rejection %		
0.001	0.5	0.9972	0.9598	3.7
0.001	1	0.5129	0.4724	7.8
0.001	2	0.3608	0.2862	20.7
0.01	0.5	0.6387	0.6954	8.1
0.01	1	0.2610	0.2476	5.1
0.01	2	0.2694	0.1971	26.8
0.1	0.5	0.5708	0.5826	2
0.1	1	0.2839	0.2574	9.3
0.1	2	0.2826	0.2045	27.6

Table 8. *Comparison of rejection values for NaCl solution (X_d = - 0.001 M, ΔP_e = 1 bar).*

C_w (M)	r_p (nm)	MENP	ENP	Error %
		Rejection %		
0.001	0.5	0.9988	0.9821	1.6
0.001	1	0.7217	0.6896	4.4
0.001	2	0.5486	0.4518	17.6
0.01	0.5	0.8209	0.8536	3.8
0.01	1	0.4476	0.4239	5.3
0.01	2	0.4310	0.321	25.5
0.1	0.5	0.7579	0.7673	1.2
0.1	1	0.4756	0.4367	8.2
0.1	2	0.4482	0.3318	26

5. CONCLUSION

In this study, linearized transport pore modeling approach is applied for modeling NF separation process. This modeling approach is based on the MENP equation improved by Debye-Huckel theory to take into account the variations of activity coefficient especially at high salt concentrations. Rejection of a single-salt (NaCl) electrolyte is investigated to investigate the effects of feed concentration, membrane charge density and pore size on variation of rejection. The results show that the reduction of feed

concentration and membrane pore size lead to an increase in rejection of electrolyte solutions in NF separation. Furthermore, increasing membrane charge density causes the rejection of co-ions to be increased leading to an enhanced total rejection. The LTPM modeling approach is compared to unmodified linearized model which shows the higher prediction of the modified model especially at higher concentrations with an error variation in the 1.5-18.9 % range.

REFERENCES

1. Wang X. L., Tsuru T., Nakao S. I., Kimura S., (1995). "Electrolyte transport through nanofiltration membranes by the space-charge model and the comparison with Teorell-Meyer-Sievers model", *J. Membr. Sci.*, 103:117-133.
2. Akbari A., Homayoonfal M., (2009). **"**Fabrication of Nanofiltration Membrane from Polysulfone Ultrafiltration Membrane Via Photo Polymerization", *Int. J. Nanosci. Nanotechnol.*, 5 (1): 43-52.
3. Ghaee A., Shariaty-Niassar M., Barzin J., Ismail A.F., (2013). "Chitosan/Polyethersulfone Composite Nanofiltration Membrane for Industrial Wastewater Treatment", *Int. J. Nanosci. Nanotechnol.*, 9 (4):213-220.
4. Mohammad A. W., Teow Y., Ang W., Chung Y., Oatley-Radcliffe D., Hilal N., (2015). "Nanofiltration membranes review: Recent advances and future prospects, *Desalination*, 356: 226-254.
5. Bowen W. R., Mohammad A. W., Hilal N., (1997). "Characterisation of nanofiltration membranes for predictive purposes-use of salts, uncharged solutes and atomic force microscopy", *J. Membr. Sci.*, 126: 91-105.
6. Hagmeyer G., Gimbel R., (1998). "Modelling the salt rejection of nanofiltration membranes for ternary ion mixtures and for single salts at different pH values", *Desalination*, 117: 247-256.
7. Schaep J., Vandecasteele C., Mohammad A. W., Bowen W.R., (1999). "Analysis of the salt retention of nanofiltration membranes using the Donnan–Steric partitioning pore model", *Sep. Sci. Tech.*, 34: 3009-3030.
8. Fievet P., Labbez C., Szymczyk A., Vidonne A., Foissy A., Pagetti J., (2002). "Electrolyte transport through amphoteric nanofiltration membranes", *Chem. Eng. Sci.*, 57: 2921-2931.
9. Mohammad A. W., Takriff M. S., (2003). "Predicting flux and rejection of multicomponent salts mixture in nanofiltration membranes", *Desalination*, 157: 105-111.
10. Kumar V. S., Hariharan K. S., Mayya K. S., Han S., (2013). "Volume averaged reduced order Donnan Steric Pore Model for nanofiltration membranes", *Desalination*, 322: 21-28.
11. Bandini S., Vezzani D., (2003). "Nanofiltration modeling: the role of dielectric exclusion in membrane characterization", *Chem. Eng. Sci.*, 58: 3303-3326.
12. Mohammad A. W., Hilal N., Al-Zoubi H., Darwish N., (2007). "Prediction of permeate fluxes and rejections of highly concentrated salts in nanofiltration membranes", *J. Membr. Sci.*, 289: 40-50.
13. Geraldes V., Alves A. M. B., (2008). "Computer program for simulation of mass transport in nanofiltration membranes", *J. Membr. Sci.*, 321: 172-182.
14. Kotrappanavar N. S., Hussain A., Abashar M., Al-Mutaz I. S., Aminabhavi T. M., Nadagouda M. N., (2011). "Prediction of physical properties of nanofiltration membranes for neutral and charged solutes", *Desalination*, 280: 174-182.
15. Roy Y., Sharqawy M. H., Lienhard J. H., (2015). "Modeling of flat-sheet and spiral-wound nanofiltration configurations and its application in seawater nanofiltration", *J. Membr. Sci.*, 493: 360-372.
16. Bowen W.R., Welfoot J.S., (2002). "Modelling the performance of membrane nanofiltration-critical assessment and model development", *Chem. Eng. Sci.*, 57: 1121-1137.
17. Bowen W. R., Welfoot J. S., Williams P. M., (2002). "Linearized transport model for nanofiltration: development and assessment", *AIChE J.*, 48: 760-773.
18. Zerafat M. M., Shariati-Niassar M., Hashemi S., Sabbaghi S., Ismail A. F., Matsuura T., (2013). "Mathematical modeling of nanofiltration for concentrated electrolyte solutions", *Desalination*, 320: 17-23.
19. Zerafat M. M. et al., (2016). Membrane Technology for Water & Wastewater Treatment, Energy & Environment, A.F. Ismail & T. Matsuura, Chapter 13: "*Mathematical modeling of nanofiltration-based deionization processes in aqueous media*", CRC Press.
20. Bowen W. R., Mukhtar H., (1996). "Characterisation and prediction of separation performance of nanofiltration membranes", *J. Membr. Sci.*, 112: 263-274.
21. Szymczyk A., Fievet P., (2005). "Investigating transport properties of nanofiltration membranes by means of a steric, electric and dielectric exclusion model", *J. Membr. Sci.*, 252: 77-88.
22. Szymczyk A., Lanteri Y., Fievet P., (2009). "Modelling the transport of asymmetric electrolytes through nanofiltration membranes", *Desalination*, 245: 396-407.
23. Saliha B., Patrick F., Anthony S., (2009). "Investigating nanofiltration of multi-ionic solutions using the steric, electric and dielectric exclusion model", *Chem. Eng. Sci.*, 64: 3789-3798.

24. Silva V., Geraldes V., Alves A. B., Palacio L., Prádanos P., Hernández A., (2011). "Multi-ionic nanofiltration of highly concentrated salt mixtures in the seawater range", *Desalination*, 277: 29-39.
25. Déon S., Dutournié P., Bourseau P., (2007). "Transfer of monovalent salts through nanofiltration membranes: A model combining transport through pores and the polarization layer", *Ind. Eng. Chem. Res.*, 46: 6752-6761.
26. Déon S., Dutournié P., Bourseau P., (2007). "Modeling nanofiltration with Nernst-Planck approach and polarization layer", *AIChE J.*, 53: 1952-1969.
27. Déon S., Dutournié P., Limousy L., Bourseau P., (2011). "The two-dimensional pore and polarization transport model to describe mixtures separation by nanofiltration: Model validation", *AIChE J.*, 57: 985-995.
28. Déon S., Escoda A., Fievet P., Dutournié P., Bourseau P., (2012). "How to use a multi-ionic transport model to fully predict rejection of mineral salts by nanofiltration membranes", *Chem. Eng. J.*, 189: 24-31.
29. Hendrix E. M., Boglárka G., (2010). "*Introduction to nonlinear and global optimization*", Springer.
30. Weise T., (2009). "*Global optimization algorithms-theory and application*".
31. Yao X., "Simulated annealing with extended neighbourhood", *Int. J. Com. Math*., 40: 169-189.
32. Ferland J. A., Hertz A., Lavoie A., (1996). "An object-oriented methodology for solving assignment-type problems with neighborhood search techniques", *Operat. Res.*, 44: 347-359.